Carbohydrate Polymers 88 (2012) 780–788

Contents lists available at SciVerse ScienceDirect

Carbohydrate Polymers

journal homepage: www.elsevier.com/locate/carbpol

Carboxylic mannan-coated iron oxide nanoparticles targeted to immune cells for lymph node-specific MRI *in vivo*

Hieu Vu-Quang[a,b,1], Muthunarayanan Muthiah[a,b,1], You-Kyoung Kim[c], Chong-Su Cho[c], Ran Namgung[d], Won Jong Kim[d], Joon Haeng Rhee[b], Sang Hyeon Kang[e], Soo Youn Jun[e], Yun-Jaie Choi[c], Yong Yeon Jeong[f], In-Kyu Park[a,b,*]

[a] *Department of Biomedical Science, Research Institute of Medical Sciences, Chonnam National University Medical School, Gwangju 501-746, South Korea*
[b] *Clinical Vaccine R&D Center, Chonnam National University Hwasun Hospital, Jeonnam 519-763, South Korea*
[c] *Department of Agricultural Biotechnology and Research Institute for Agriculture and Life Sciences, Seoul National University, Seoul 151-921, South Korea*
[d] *Department of Chemistry, BK School of Molecular Science, Polymer Research Institute, Pohang University of Science and Technology, Pohang 790-784, South Korea*
[e] *iNtRON Biotechnology, Inc., Seongnam 462-120, South Korea*
[f] *Department of Radiology, Chonnam National University Hwasun Hospital, Jeonnam 519-763, South Korea*

ARTICLE INFO

Article history:
Received 20 December 2011
Received in revised form 12 January 2012
Accepted 20 January 2012
Available online 28 January 2012

Keywords:
Carboxylic mannan
Mannose receptor
Superparamagnetic iron oxide nanoparticles
MR imaging
Lymph node

ABSTRACT

Carboxylic mannan (CM)-coated super paramagnetic iron oxide nanoparticles (CM-SPIONs) were prepared to target antigen-presenting cells (APCs), including macrophages, by the specific interaction between the mannose ligand tethered on CM-SPION and mannose receptors on APCs. Carboxylic mannan was synthesized by introducing the aldehyde group to mannan by oxidation, followed by the conversion of aldehyde groups to carboxyl groups. CM-SPION exhibited uniform-sized nanoparticles with a highly negative surface charge appropriate for longer blood circulation. It was demonstrated that CM-SPION could target macrophages bearing mannose receptors more specifically than polyvinyl alcohol (PVA) or dextran-coated SPION. The *in vitro* and *in vivo* toxicities of CM-SPION were evaluated, and the results showed that the LD_{50} of CM-SPION was much higher than that of mannan-SPION (80 mg Fe/kg *vs.* 44 mg Fe/kg in mice, respectively). The uptake of CM-SPION by peritoneal macrophages was also confirmed with Prussian blue staining and magnetic resonance (MR) phantom tube imaging. In the *in vitro* uptake study visualized by MR phantom tube imaging, the intracellular uptake of CM-SPION was much faster than those of dextran-coated SPION (Dex-SPION) and PVA-coated SPION (PVA-SPION) at the initial hours of incubation, and increased drastically up to 24 h post-incubation. The *in vivo* uptake of CM-SPION in lymph nodes (LNs) was tracked by MR imaging (MRI) after subcutaneous injection in a rat model. It was found that the injected CM-SPION predominantly accumulated in the popliteal LN, and the *in vivo* accumulation rate with CM-SPION in the LN was comparable to that of Dex-SPION, the positive control, as measured by a signal drop in MR intensity. Histological analysis with Prussian blue staining also confirmed the accumulation of SPION in the LN.

1. Introduction

Superparamagnetic iron oxide nanoparticles (SPIONs) have been used as a contrast agent in magnetic resonance imaging (MRI) or as a carrier platform in the applications of drug (Butoescu, Seemayer, et al., 2009; Butoescu, Jordon, et al., 2009; Munnier et al., 2008) and gene delivery (Lee, Kim, Kim, & Kim, 2002; Ran et al., 2010). SPIONs can be synthesized by different methods, including co-precipitation, reaction in constrained environments, thermal decomposition, sol–gel reaction, polyol methods, aerosol/vapor methods, and sonolysis (Laurent et al., 2008). To increase its stability, SPION has been coated by many kinds of hydrophilic materials such as dextran, polyethylene glycol (PEG), poly-vinyl alcohol (PVA), chitosan, and others (Chastellain, Petri, & Hofmann, 2004; Lee et al., 2002; Liu et al., 2011; Lu, Yin, Mayers, & Xia, 2002; Petri-Fink, Chastellain, Juillerat-Jeanneret, Ferrari, & Hofmann, 2005; Schöpf et al., 2005; Shen, Weissleder, Papisov, Bogdanov, & Brady, 1993). However, SPION medical applications are limited due to several problems such as aggregation, toxicity, and lack of tissue specificity during systemic circulation (Gupta & Gupta, 2005; Lin, Lee, & Chiu, 2005; Neenu, Gareth, Romisa, & Shareen, 2010).

The properties of nanoparticles can be significantly altered by surface modification. The typical approach to tailoring the surface

* Corresponding author at: Department of Biomedical Science, Research Institute of Medical Sciences, Chonnam National University Medical School, Gwangju 501-746, South Korea. Tel.: +82 61 379 8481; fax: +82 61 379 8455.
E-mail addresses: pik96d@gmail.com, pik96@chonnam.ac.kr (I.-K. Park).
[1] These two authors have equally contributed to this work.

0144-8617/$ – see front matter © 2012 Elsevier Ltd. All rights reserved.
doi:10.1016/j.carbpol.2012.01.067

properties of nanoparticles is mediated by surface coating or encapsulation with biocompatible materials (Caruso & Antonietti, 2001). Besides improving its durability and suspensibility in biological environments, and its biocompatibility, the functional coating on the surface of nanoparticles can also be used to immobilize or tailor the bio-distribution of foreign molecules (Bucak, Jones, Laibinis, & Hatton, 2003). The surface coating of SPION has helped to resolve its drawbacks encountered in *in vivo* with unmodified SPION. The carboxyl group has been introduced as a surface coating for SPION, and this approach has been shown to have many advantages (Yu & Chow, 2004). Negatively charged SPION usually has the free carboxyl group on its surface, and this can be utilized for covalent attachment with proteins and other therapeutic molecules. The carboxyl group can also improve the dispersion of iron oxide nanoparticles in a biological system by improving the hydrophilicity (Yu & Chow, 2004). Negatively charged nanoparticles have less chance of interacting with the negatively charged plasma membrane of the cells and the negatively charged proteins encountering during circulation before reaching the target tissue; this results in increased systemic circulation (He, Hu, Yin, Tang, & Yin, 2010).

Targeting to specific cells or tissue is an important issue for the medical application of nanoparticles. For instance, SPION coated with polyvinylbenzyl-*O*-β-D-galactopyranosyl-D-gluconamide (PVLA)-galactose moieties can be targeted to hepatocytes *via* asialoglycoprotein receptors, which allows for the enhanced MR contrast imaging of the rat liver after intravenous administration (Yoo et al., 2007). Moreover, dextran-coated SPION (Dex-SPION) has been approved in clinical trials as an MRI contrast agent with commercial names such as Lumirem, Endorem, and Sinerem. Dex-SPION could be targeted to macrophages through scavenger receptors, which have been already used for the diagnosis of metastatic liver and metastatic LN in MRI (Bellin et al., 1994; Corot, Robert, Idée, & Port, 2006; Harisinghani et al., 2003; Raynal et al., 2004). Carboxy dextran SPION (SH U 555 A, RESOVIST) has also been approved in clinical trial settings as a faster contrast agent for liver MRI (Reimer & Balzer, 2003). The compound can be regarded as safe and well tolerated. Even bolus injections cause no cardiovascular side effects, lumbar back pain, or clinically relevant laboratory changes. It also prevents nanoparticle aggregation and makes magnetic nanoparticles highly hydrophilic (Reimer & Tombach, 1998). It is also reported that dextran SPION accumulates in the LN after local injection. Once it reaches the LN, it is trapped by the immune cells in the LN (Mehvar, 2000).

It was previously reported that mannan-coated SPION (mannan-SPION) could be specifically targeted to macrophages by the interaction with mannose receptors on antigen-presenting cells (APCs) (Yoo et al., 2008). Mannan is a cell wall component of microorganisms, consisting of D-mannose residues expanded by a-(1,6)-, a-(1,3)-, and a-(1,2)-linkages. Mannan is also recognized by the mannose receptors of APCs and reticuloendothelial cells, which mainly reside in the normal LN. In our previous study, it was also demonstrated that mannan-SPION was specific to immune cells in LN due to mannose receptor-mediated endocytosis, facilitating preferential uptake in APCs and achieving faster acquisition and enhanced contrast of MR imaging in target tissue as compared with Dex-SPION and PVA-coated SPION (PVA-SPION) (Vu-Quang et al., 2011). It was also previously reported by our group that SPION coated with β-glucan could target APCs, since glucan was reported to elicit immune responses through the activation of macrophages with an immune cell-specific (1,3)-β-D-glucan receptor or dectin-1 receptor. β-Glucan-coated SPION was internalized by the immune cells residing in the metastatic liver, which aided in discrimination between metastasized tumor regions and normal hepatic parenchymal tissue. β-Glucan also induces the immune system, which aids in anti-tumor activity (Vu-Quang et al., 2012). However, the direct exposure of immune cells to a higher molecular yeast mannan component coated on mannan-SPION might cause severe immune responses after administration (Ataoglu, Dogan, Mustafa, & Akarsu, 2000). It has been hypothesized that the carboxylation of mannan coated on the surface of iron oxide nanoparticles might reduce this toxic response. Thus, carboxylic mannan-coated SPION (CM-SPION) was synthesized by introducing the carboxyl group to mannan with periodate/sodium chlorite reactions. Following this, the carboxylic mannan was coated on SPION in order to alleviate the systemic toxicity caused by the direct exposure to higher molecular mannan. We investigated the physicochemical properties, the *in vitro* and *in vivo* uptakes of CM-SPION using MRI and assessment of systemic toxicity. This uptake was also confirmed with Prussian blue staining.

2. Materials and methods

2.1. Materials

Mannan from *Saccharomyces cerevisiae* was purchased from Sigma–Aldrich Chemical Co. (MO, USA). Hydroxyl-amine hydrochloride, 2,4-dihydroxy-benzaldehyde, and sodium chlorite were also purchased from Sigma–Aldrich. Sodium periodate, ethylene glycol, and hydrogen peroxide solution were purchased from Samchun Chemicals (South Korea). The dialysis membrane (MWCO 1000 Da) was purchased from Spectrum Laboratories (Rancho Dominguez, CA, USA).

2.2. Carboxylation of mannan

To introduce aldehyde groups onto mannan, mannan was oxidized following the standard methods with minor modifications (Massia & Stark, 2001; Mislovičová, Masárová, & Gemeiner, 2001). Mannan (400 mg, 2.3 mmol mannose) was dissolved in 16 mL of distilled water (DW); then, sodium periodate solution (0.1 M, 0.45 mmol or 0.90 mmol) was slowly dropped into the solution under continuous stirring at 4 °C in the dark for 1 h. The oxidation reaction was stopped by adding ethylene glycol (0.9 mmol or 1.8 mmol) and stirred for another 30 min. The oxidized mannan was purified by dialysis using a dialysis membrane (MWCO 1000 Da) against DW at 4 °C for 1 day. The purified oxidized mannan was then lyophilized to obtain a white solid and kept at 4 °C.

The number of aldehyde groups of mannan was quantitatively analyzed using the standard protocol with a slight modification (Zhao & Heindel, 1991). Aldehyde-mannan (11 mg) was dissolved in hydroxyl-amine hydrochloride solution (0.25 M, 5 mL) with a pH of 2.14. The solution was sonicated for 2 h and stored overnight at room temperature. Degree of aldehyde groups of oxidized mannan was determined by titration of the HCl, which was generated by treating the aldehyde functionality with a measured amount of hydroxylamine hydrochloride. The titration was performed using NaOH (0.1 M) solution until the end point was reached at pH 2.14. Finally, the amount of aldehyde groups in the mannan was calculated by comparing the titer value of NaOH against the amount in 2,4-dihydroxy-benzaldehyde, a standard aldehyde reagent for this titration method. The degree of aldehyde functionalization on the mannose ring was estimated to be 19% or 29%.

To convert the aldehyde groups to carboxylic acid groups, aldehyde mannan was oxidized using sodium chlorite (Haaksman, Besemer, Jetten, Timmermans, & Slaghek, 2006; Raach & Reiser, 2000). Aldehyde mannan (340 mg, 19% ring-opened mannose or 370 mg, 29% ring-opened mannose) was dissolved in 20 mL DW and hydrogen peroxide (1.2 equiv. to mannose ring) was added in an ice bath. Then, sodium chlorite solution (0.5 M, 1.2 equiv. to mannose ring) was slowly dropped into the solution and the pH was adjusted to 5. After removal from the ice bath, the mixture was stirred and

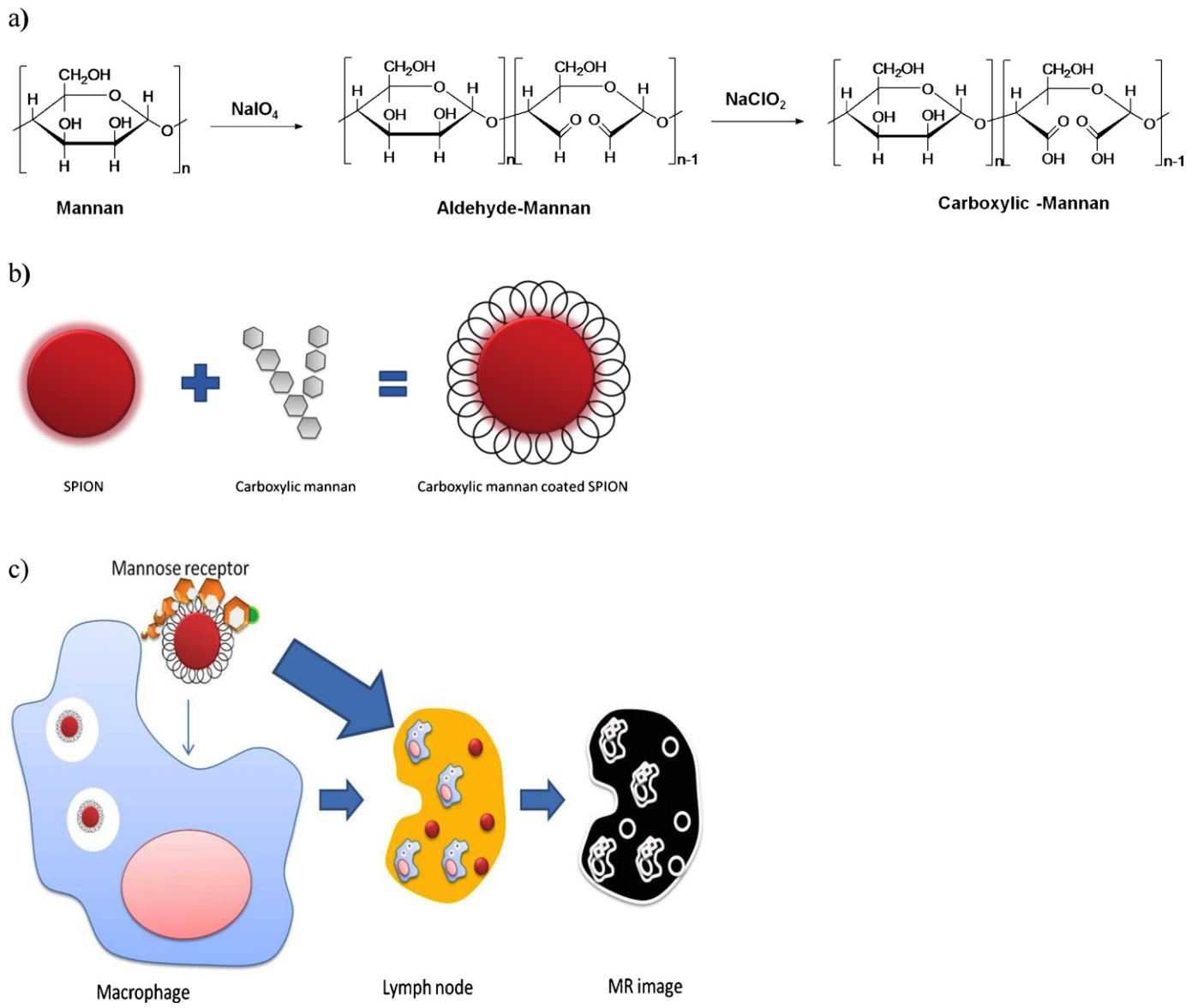

Scheme 1. Synthesis of CM-SPION targeted to immune cells in LN. (a) CM synthesis process. The mannan sugar ring was replaced by aldehyde at carbon positions number 2 and 3. Then, aldehyde-mannan was converted to carboxylic mannan by oxidation. (b) Preparation of CM-coated SPION. (c) CM-SPION was recognized by the mannose receptor of the macrophage. After subcutaneous injection of the contrast agent in the foot pad, CM-SPION would diffuse directly to the LN near the site of injection. Once it reached the LN, it would be trapped by the immune cells present in the LN. In MRI, CM-SPION gives a negative enhancement effect in T2-weighted images.

maintained at pH 5 by the addition of NaOH solution. When the rate of consumption of NaOH was negligible, the pH was adjusted to 9. The product was purified by dialysis using a dialysis membrane (MWCO 1000 Da) against DW at 4 °C for 1 day and lyophilized.

The amount of carboxylic acid groups in the mannan was quantitatively analyzed by acid–base titration using 1 M HCl solution. As a result, 10% or 13% of the mannose ring was converted to carboxylated mannose.

2.3. Synthesis of CM-SPION

The CM-SPION was synthesized, with some modifications, according to a previous publication (Yoo et al., 2008). Following the addition of NH_4OH, SPION was prepared by alkaline co-precipitation of $FeCl_3{\cdot}6H_2O$ and $FeCl_2{\cdot}4H_2O$ (Sigma–Aldrich) with a Fe(III)/Fe(II) feed ratio of 3:1 in the deoxygenated water. The black precipitate was washed multiple times and the final pH was adjusted from 10 to 7. The solution was allowed to sediment under a magnetic field and the supernatant was discarded. The black sediment was mixed with 2 M HNO_3 and 0.35 M $Fe(NO_3)_3$. The suspension was dialyzed for 2 days against 0.01 M HNO_3, and stored at 4 °C. Finally, the product was co-incubated with carboxylic mannan in order to obtain CM-SPION, and the pH was adjusted to 7 using NH_4OH. The other contrast agents, Dex-SPION and PVA-SPION, were prepared using the same method.

2.4. Characterization of CM-SPION

The sizes of SPIONs were assessed at 25 °C using an electrophoretic light scattering spectrophotometer (ELS 8000, Otsuka Electronics, Osaka, Japan) with 90° and 20° scattering angles. Electrophoretic mobility was measured using the same setup equipped with a platinum electrode. Fourier-transform infrared (FT-IR) spectra were acquired using a VERTEX 70 FT-IR (Bruker Optics GmbH, Germany). The transmittance of pellets consisting of carboxylated mannan (or mannan, aldehyde-mannan) and KBr was measured

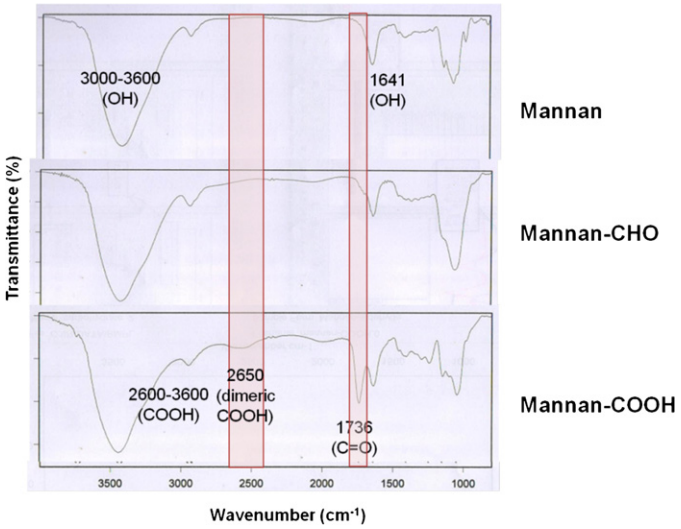

Fig. 1. FT-IR spectra of mannan, mannan-aldehyde (CHO), and mannan-COOH. A broad band at 2650 cm^{-1} confirmed the presence of dimeric COOH. A narrow band at 1736 cm^{-1} confirmed the presence of the carbonyl (C=O) group in the mannan-COOH.

at a wavenumber interval of 800–4000 cm^{-1}. The morphology of CM-SPION was characterized by transmission electron microscopy (TEM) (JEOL JEM-2000 FX-II, Japan).

2.5. Primary peritoneal macrophage isolation

Three days after intraperitoneal injection of 3 mL Brewer thioglycolate medium into inbred Balb/c 7-week-old male mice (Orient Bio Inc., Seongnam-si, South Korea), peritoneal macrophages were collected by two injections of 7 mL of serum-free ice cold RPMI 1640 (Thermo Scientific, UT, USA) into the peritoneal cavity. The fluid was collected, centrifuged, treated with ACK buffer (Lonza Walkersville, MD, USA) for 5 min, and washed with PBS three times at 1000 rpm for 10 min. Cells were allowed to adhere to the cell culture dish for 2 h in serum-free RPMI 1640 in a 5% CO_2 atmosphere at 37 °C. The dish was then washed three times with cold PBS to remove non-adherent cells. Adherent cells were harvested with a cell scraper.

2.6. In vitro cytotoxicity of CM-SPION

Isolated peritoneal macrophages were seeded in 96 well plates at a density of 2×10^4/well in 100 μL of RPMI 1640 growth medium and incubated overnight at 37 °C in 5% CO_2. The cells were treated with CM-SPION, Dex-SPION, and PVA-SPION at various concentrations (5, 25, 50, and 100 μg Fe/mL) for 24 h. The cells were then incubated with 100 μL of MTT solution for 4 h to allow formation of formazan crystals by mitochondrial dehydrogenases. The medium was removed and 100 μL of DMSO was added to dissolve the formazan crystals. The optical density of the solution was measured at a wavelength of 570 nm using a Spectra Max 190 spectrophotometer (Molecular Devices, Sunnyvale, CA, USA).

2.7. In vitro uptake of CM-SPION in peritoneal macrophages

Macrophages were harvested and cultured with a cell density of 5×10^5 cells/well in a 24-well plate in 500 μL of RPMI 1640 growth medium. The macrophages were incubated with the determined amount of CM-SPION (iron conc. 100 μg Fe in each well). At 3 and 24 h post-incubation, the treated macrophages were harvested, washed three times with PBS, and then fixed with 4% HCHO. The fixed macrophage cells were stained with Prussian blue. The intracellular accumulation of CM-SPION by mouse peritoneal macrophages was evaluated semi-quantitatively by MRI. The fixed cells were counted again and embedded in 10% gelatin (1:1). Next, the middle gelatin layer was placed in 0.5 mL Eppendorf tubes for *in vitro* phantom MRI measurements. The MR phantom tubes were placed in a water bath inside the magnetic field (b0) of an MRI machine. MRI scanning was performed with a 3.0 T clinical whole-body MR unit (Siemens Magneto Tim Trio 3.0 T, wrist coil). The MR sequence was a two-dimensional (2D) gradient-echo sequence with TR = 3000, TE = 75, NEX = 4, slice thickness = 2 mm, flip angle = 150°, and field of view (FOV) = 214 × 384.

2.8. Systemic toxicity of CM-SPION

Toxicological comparison was performed between CM-SPION and mannan-SPION using the conventional single-dose intravenous toxicity test. The test was performed at the Korea Institute of Toxicology, Korea Research Institute of Chemical Technology. Particularly, CM-SPION or mannan-SPION was administered to 7-week-old ICR mice (five male mice and five female mice per group) at different doses of 20, 40, and 80 mg Fe/kg by intravenous injection. General symptoms, deaths, and weight changes in mice were observed for 15 days. Then, any abnormal signs in the internal organs were checked by autopsy. All experiments were performed after approval by our local ethical committee at the Chonnam National University Medical School (CNU IACUC-H-2011-5) and in accordance with the principles of laboratory animal care (NIH publication #85-23).

2.9. Magnetic resonance imaging

In the case of *in vivo* MRI study, SPF/VAF outbred rats (7 weeks, male) (Orient, Seongnam, South Korea) and Balb/c mice were immobilized with isofurane 2% (Choongwae, Seoul, South Korea) and pre-scanned using clinical MRI equipment (Siemens wrist coil for rats and Siemens volume coil for mice) on the hind and inguinal LN area. All experiments were performed after approval by our local ethical committee at the Chonnam National University Medical School and in accordance with the principles of laboratory animal care (NIH publication #85-23). MRI was used to assess the accumulation of the SPION in the LNs. The scanning protocol included the acquisition of T2-weighted spin echo coronal images for localization of the LN (measured parameters: slice thickness 1 mm, matrix 256 × 218, TR = 3000 ms, NEX = 2, TE = 104 ms, 1 average, FOV 100 mm × 100 mm, and flip angle = 150°). Immediately after pre-scanning, CM-SPION of 12.5 mg Fe/kg (five rats in each group) was injected into the rats; they were scanned after 1, 2, 3, and 24 h in the same locations. In the case of metastatic LN mouse models, CM-SPION was subcutaneously injected in the footpad with 12.5 mg Fe/kg and scanned after 24 h. The mice were sacrificed after the last scan. Signal intensities from the muscle region and LN were measured and converted to the relative intensity ratio between the LN and muscle. The signal intensity ratio from the pre-scanning imaging was set at 100%.

2.10. Histological analysis with Prussian blue staining

Paraffin blocks were prepared from the fixed peritoneal macrophages and tissue samples and processed for Prussian blue staining. Each paraffin-embedded sample was sliced into 5 μm sections, which were placed on glass slides. The sections were deparaffinized and serially hydrated by immersing the slides twice in 100% xylene, twice in 100% ethanol, and once in 95%, 90%, 80%, and 70% ethanol. The hydrated slides were washed under tap water for 5 min and stained with a 1:1 mixture of 20% HCl and 10% potassium

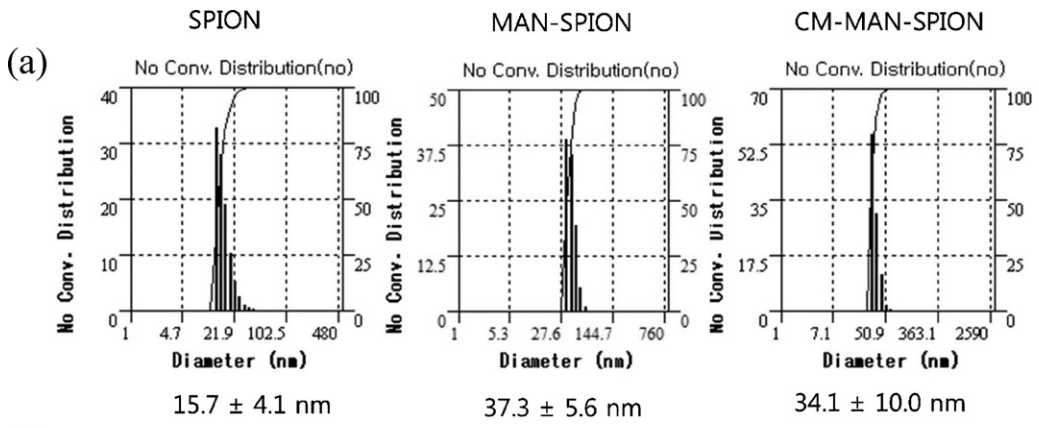

(b)

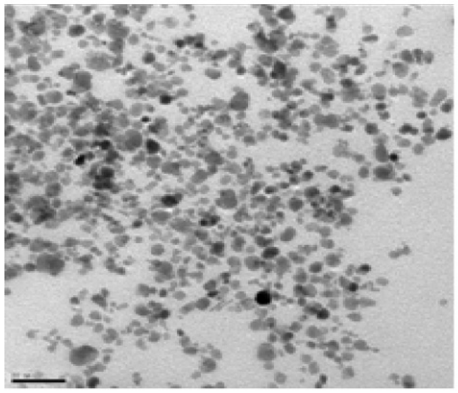

(c)

	DLS size (nm)	Zeta potential (mV)
SPION	15.7±4.1	4.44±3.51
Mannan SPION	37.3±5.6	-8.88±6.96
CM-SPION	34.1±10	-31.69±2.52

Fig. 2. Physicochemical characterization. Size distribution by dynamic light scattering (DLS) (a). The hydrodynamic radii of SPION, mannan-SPION, and CM-SPION were found to be 15, 37, and 34 nm, respectively. (b) TEM image of CM-SPION showing the morphology of the nanoparticles. Scale bar: 200 nm. (c) Average sizes and surface charges of SPION, mannan-SPION, and CM-SPION measured by DLS and Zeta potential analyses.

ferrocyanide trihydrate for 20 min. The slides were then counterstained with Nuclear Fast Red solution (Sigma–Aldrich) for 5 min. The stained slide was mounted in Permount solution (Fisher Scientific, PA, USA).

2.11. Statistical analysis

Quantitative data are expressed as means ± standard deviation (SD). The means were compared using an independent samples *t*-test. *P* values less than 0.05 were considered statistically significant.

3. Results and discussion

3.1. Preparation of carboxylic mannan (CM)

Firstly, the aldehyde group was introduced to mannan by oxidation; then, the resulting aldehyde groups were converted to the carboxyl group. To convert aldehyde groups to carboxylic acid groups, aldehyde mannan was oxidized using sodium chlorite (Scheme 1a). The amount of carboxylic acid groups in the mannan was quantitatively analyzed by acid–base titration. Ten to 13% of the aldehyde group was introduced in the D-mannose ring of mannan and then converted to the carboxyl group, while more than 80% of D-mannose remained intact, which would help in targeting to the specific receptors on immune cell surfaces.

The CM was analyzed through FT-IR (Fig. 1) to confirm the introduction of the carboxyl group to mannan. In the wavenumber range corresponding to COOH (2600–3600 cm^{-1}), the appearance of a broad band at 2650 cm^{-1} confirmed the presence of dimeric COOH. There was also a narrow band at 1736 cm^{-1}, indicating the presence of the carbonyl (C=O) group in the carboxylic mannan. It was clear from the FT-IR data that the carboxyl group was successfully introduced to the mannan carbohydrate.

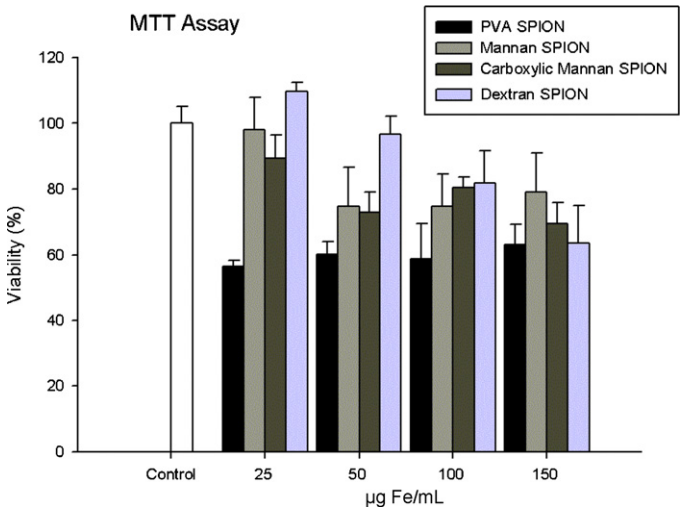

Fig. 3. Cytotoxicity assay of PVA-SPION, mannan-SPION, CM-SPION, and Dex-SPION concentration (25, 50, 100, and 150 μg/mL). Peritoneal macrophages were seeded at a concentration of 2 × 104 cells in 96-well plates. Macrophages were incubated with contrast agents at various iron concentration (25, 50, 100, and 150 μg Fe/mL) for 24 h.

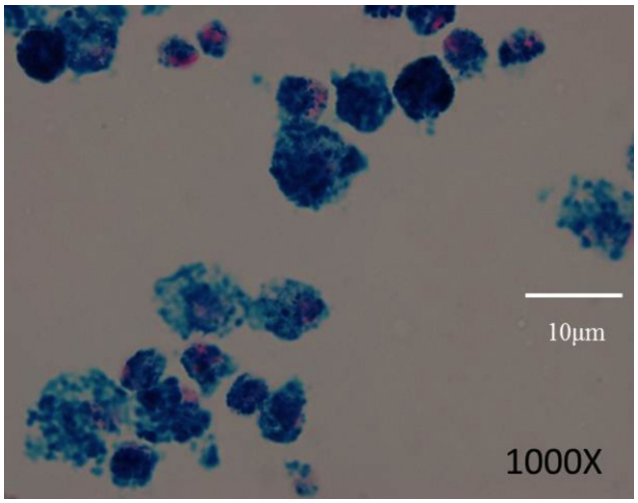

Fig. 4. Intracellular uptake of CM-SPION by peritoneal macrophages isolated from Balb/c mice. The cells were incubated with CM-SPION for 3 h. Prussian blue staining: blue: SPION; red: nucleus. magnification 1000×. (For interpretation of the references to color in this figure legend, the reader is referred to the web version of the article.)

3.2. Synthesis of CM-SPION

SPION was coated with CM to create a well-dispersed iron oxide solution that can be targeted to macrophages *via* the mannose receptor. SPION was synthesized using an alkaline co-precipitation method, followed by surface coating of SPION with CM carbohydrate; the resulting CM-SPION was subsequently investigated for immune cell-specific internalization using LN-specific MRI (Petri-Fink et al., 2005). Hydrogen bonding is assumed to be the predominant mechanism for the adsorption of a hydrophilic polymer such as carboxyl mannan onto the oxide surface of magnetic nanoparticles, which occurs through the interaction between the polar functional groups of carboxyl mannan and the hydroxylated and/or protonated ones of the iron oxide nanoparticles (Chastellain et al., 2004; Yamaura et al., 2004).

3.3. Characterization of CM-SPION

The size of CM-SPION was measured by Dynamic light scattering (DLS). The particle sizes of SPION before and after coating with carboxylic mannan were around 15.7 ± 6.3 nm and 34.1 nm ± 10, respectively (Fig. 2). Zeta potential measurement revealed surface charges of the uncoated SPION and CM-SPION of approximately +4.44 ± 3.5 mV and −31.69 ± 2.5 mV, respectively (Fig. 2). The negatively charged CM-SPION can protect nanoparticles efficiently from unwanted and premature agglomeration with negatively charged biocomponents, including red blood cells, before reaching the target. Therefore, it might be safer for the recipient patients during diagnosis. The specific binding of the carrier to APCs including macrophages is possibly due to the mannose exposed on the CM-SPION. The morphology of CM-SPION was analyzed through TEM; the nanoparticles exhibited uniformly spherical morphology with a narrow distribution range in diameter (Fig. 2).

3.4. In vitro cytotoxicity of CM-SPION

CM-SPION, PVA-SPION, and Dex-SPION at various concentrations were treated with murine peritoneal macrophage cells and the cellular viability after the treatment with those SPIONs was analyzed by MTT assay. CM-SPION was compared with PVA-SPION, and Dex-SPION. Dex-SPION has been used as the commercially available contrast agent and PVA-SPION have already been shown to have good biocompatibility and internalization capacity (Vu-Quang et al., 2012). Thus, they were chosen for comparison in this study. Fig. 3 shows the MTT assay results for the cytotoxicity of these SPIONs against murine peritoneal macrophage cells isolated from the peritoneal cavity. When the iron concentration was increased, the cell viability of the CM-SPION-treated group was minimally affected, indicating that CM-SPION displayed a cytotoxicity level similar to that of Dex-SPION, a contrast agent currently used in clinical diagnosis, and a lower cytotoxicity than PVA SPION. Thus, CM-SPION appears to be useful as a nontoxic contrast agent for MRI.

3.5. In vitro uptake of CM-SPION

Intracellular residence of the particles was validated by Prussian blue staining. The blue dots indicate the presence of iron inside the macrophage and the pink represents the nucleus. The

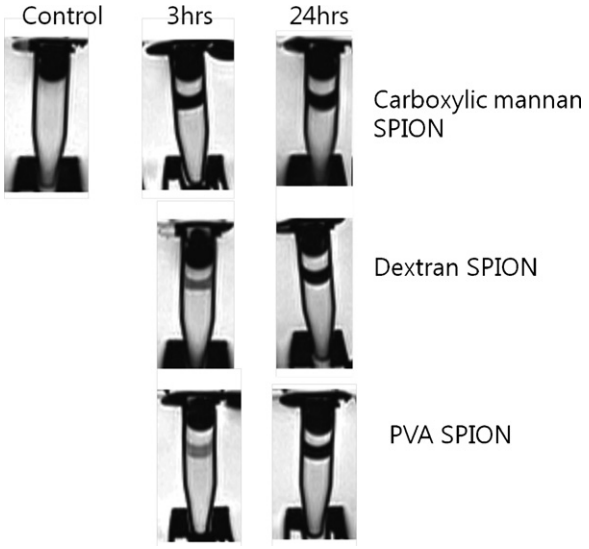

Fig. 5. MR phantom tube imaging of CM-SPION, Dex-SPION, and PVA-SPION after incubation with peritoneal macrophages for 3 h and 24 h. Cells (2×10^5) were immersed in 5% gelatin and cell-containing gel was found in the middle layer of the microcentrifuge tube.

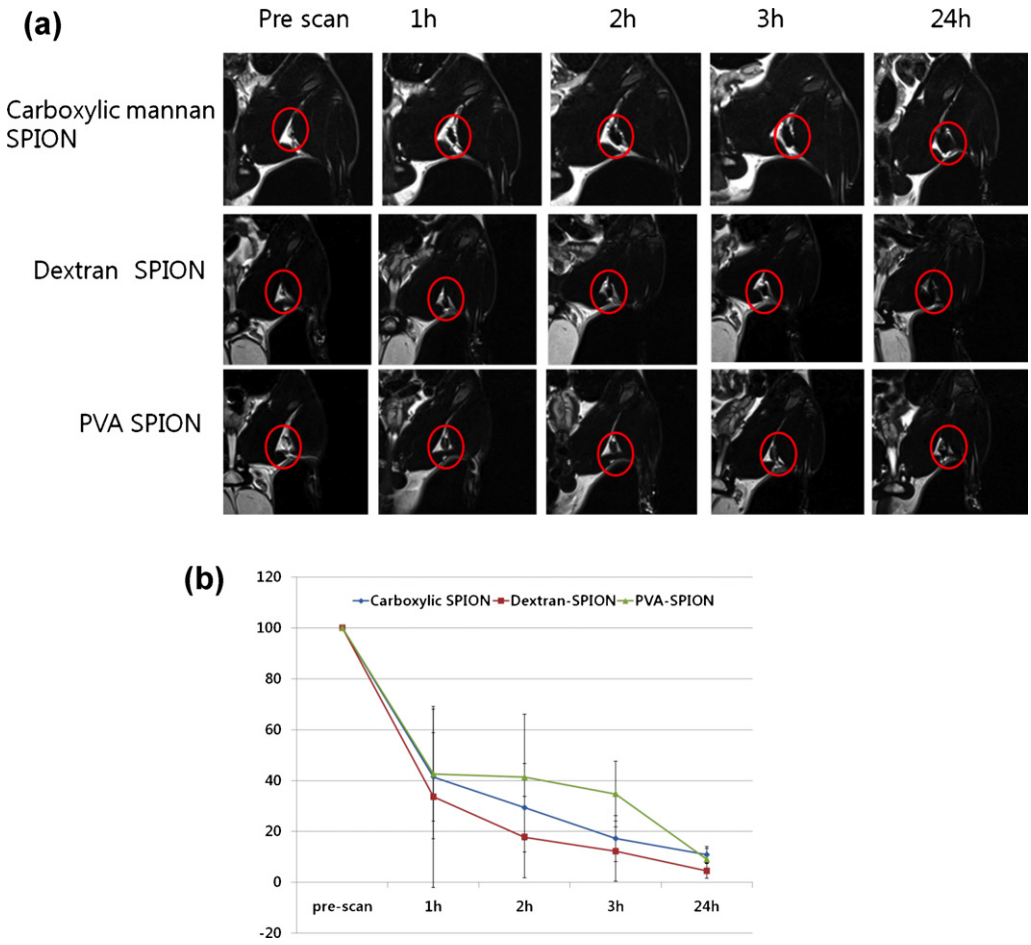

Fig. 6. Time-dependent MR imaging (a) and signal intensity profile (b) in popliteal LN after local injection in the foot pad. Rats were injected with CM-SPION, Dex-SPION, and PVA-SPION (12.5 mg Fe/kg Rat) in the foot pad subcutaneously. They were scanned before injection and 1, 2, 3, and 24 h after subcutaneous injection. A drop in signal intensity was recorded as a ratio of LN to back muscle, and the ratio at pre-scan was set to 100%. (a) MR LN-imaging at pre-scan, 1, 2, 3, and 24 h and (b) signal intensity ratios ($n = 5$).

cells were treated with CM-SPION, PVA-SPION, and Dex-SPION (Fig. 4) and stained with Prussian blue 3 h after the treatment to analyze the intracellular uptake of the SPION particles by the respective cells. The particles were clearly recognized and phagocytosed by peritoneal macrophages. The intracellular accumulation of CM-SPION in macrophages was higher than those of either PVA-SPIONs or Dex-SPIONs. The intracellular localization of CM-SPIONs was observed in the cytoplasm of these cells, which is visible in Fig. 4.

The macrophage cells were treated with CM-SPION, PVA-SPION, and Dex-SPION and placed between two gelatin layers. The MR signal drop from the phantom tubes containing the macrophage cells treated with respective SPION particles was analyzed according to time course post-incubation, as shown in Fig. 5. At 3 h post-incubation, a significant drop in MR signal intensity was noted for the phantom tube containing the macrophages incubated with CM-SPION. This indicated a preferential uptake of CM-SPION by macrophages compared to PVA-SPION and Dex-SPION, which was possibly a result of specific interaction between the carboxylated mannan on the CM-SPION and specific receptors such as dectin-1 on the macrophage cells. Receptor-targeted uptake by macrophages was rapid, which was also demonstrated in our previous publication, where the mannose receptor on macrophages was successfully targeted with mannan-SPION. A highly facilitated uptake of mannan-coated SPION into macrophages was found when compared to those of Dex-SPIONs and PVA-SPIONs (Vu-Quang et al., 2011).

3.6. Systemic toxicity of CM-SPION

CM-SPION or mannan-SPION was administered to 7-week-old ICR mice (five male mice and five female mice per group) at different doses of 20, 40, and 80 mg Fe/kg by intravenous injection. The mice administered with mannan-SPION at the dose of at least 20 mg Fe/kg died or demonstrated subdued behavior, irregular respiration, prone position, and lower abdomen contamination. A 50% lethal dose (LD_{50}) of mannan-coated SPION was determined to be 44 mg Fe/kg in both male and female mice (Table 1). The mice administered with CM-SPION showed no abnormality; both male and female mice were safe after the injection and observation period. The LD_{50} of CM-SPION was more than 80 mg Fe/kg in mice (Table 1). This result indicates that CM-SPION is a much safer MRI contrast agent than mannan-coated SPION.

3.7. In vivo macrophage targeting

In MRI, T2-weighted gradient echo imaging is a useful option to evaluate the accumulation of SPION *in vivo*. Normal rats were

Table 1
Systemic toxicity of mannan-SPION and CM-SPION after the administration to 7-week-old ICR mice. Systemic toxicity was expressed as an LD_{50} value in mg/kg.

	LD_{50} (mg/kg)
Mannan-SPION	44
CM-SPION	80

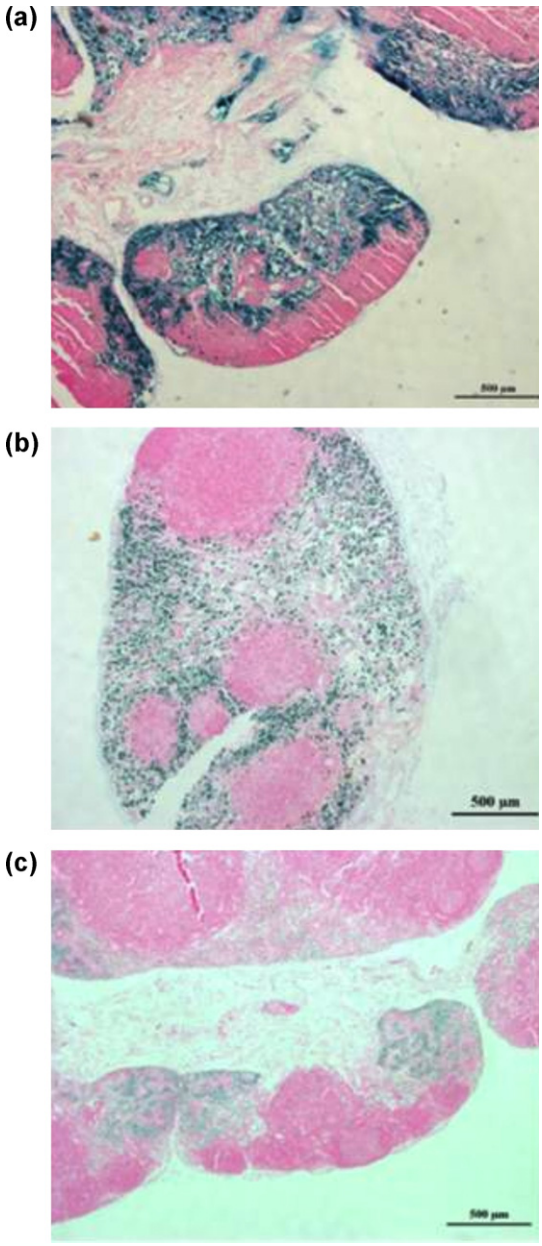

Fig. 7. Prussian blue staining of LN injected with CM-SPION (a), Dex-SPION (b), and PVA-SPION (c). After 24 h of local injection, rats were sacrificed and popliteal LN near the injection site on the same leg was taken out. LN was sectioned and stained with Prussian blue. Blue indicates iron, pink: nucleus fast red. (For interpretation of the references to color in this figure legend, the reader is referred to the web version of the article.)

used to investigate the macrophage targeting ability of CM-SPION as an MRI contrast agent. It was expected that the CM-SPION could be targeted to the mannose receptor expressing on APCs, including macrophages residing in the LN. After subcutaneous injection of the contrast agent in the foot pad, CM-SPION would diffuse directly to the LN near the site of injection. Once it reached the LN, it would be trapped by the immune cells present in the LN (Harisinghani et al., 2003) as described in Scheme 1c. The T2-weighted MR image after subcutaneous injection of CM-SPION is shown in Fig. 6a. The signal intensity of the LN on T2-weighted MRI after injection of the contrast agent was negatively enhanced compared to that of T2-weighted MR images of the same LN before injection. According to the quantitative analysis shown in Fig. 6b, the negative enhancement in MR signal on LN, represented as LN-to-muscle ratio, showed a drastic signal drop (darkening) of $41 \pm 17\%$ at 1 h after injection of CM-SPION. On the other hand, PVA- and Dextran-SPION also exhibited a signal drop of around 40.0%, similar to that of CM-SPION. In the presence of SPION, the signal in the T2-weighted sequence becomes darker (negative contrast) due to the shortening of proton spin. The CM-SPION was mainly accumulated in the popliteal LN after subcutaneous injection in the foot pad. The signal drop in MR intensity of CM-SPION was equivalent to that of Dex-SPION, the commercially available contrast agent, and was more enhanced than that of PVA-SPION, even from the initial hours up to 24 h. The accumulation of SPION in the LN was also confirmed by Prussian blue staining, as shown in Fig. 7. The blue dots indicate the presence of iron inside the macrophage and the pink represents the nucleus. From the histological analysis, it is evident that the accumulation of CM-SPION is more enhanced than that of PVA-SPION and Dex-SPION. There was uniform and dense distribution of CM-SPION found in the LN compared to PVA-SPION and Dex-SPION. The dense distribution might help in prominent LN MR imaging, making the detection of micro-metastasis easier.

4. Conclusion

CM-SPION was synthesized to target immune cells expressing mannose receptors on the cell surface, achieving longer circulation than mannan-SPION without compromising specificity. The intracellular accumulation of CM-SPION in macrophages was higher than those of either PVA-SPIONs or Dex-SPIONs. The intracellular localization of CM-SPIONs was pre-dominantly observed in the cytoplasm of APCs. CM-SPION represented reduced systemic toxicity compared to mannan-SPION, and still possessed enhanced accumulation similar to Dex-SPION in LN after local administration. Our data suggest that CM-SPION can be regarded as a safe and potential contrast agent in LN-targeted MR imaging.

Acknowledgements

This work was financially supported by the Bio Imaging Research Center at GIST. IKP also acknowledges the financial support of the Regional Technology Innovation Program of the Ministry of Commerce, Industry and Energy (Grant RT104-01-01); the Basic Science Research Program through the National Research Foundation of Korea, funded by the Ministry of Education, Science and Technology (2010-0002940); the Korea Healthcare Technology R&D Project, Ministry for Health, Welfare & Family Affairs, Republic of Korea (A084869 and A100553); the Leading Foreign Research Institute Recruitment Program through the National Research Foundation of Korea (NRF), funded by the Ministry of Education, Science and Technology (MEST) (2011-0030034); the Small and Medium Business Administration of Korea.

References

Ataoglu, H., Dogan, M. D., Mustafa, F., & Akarsu, E. S. (2000). *Candida albicans* and *Saccharomyces cerevisiae* cell wall mannans produce fever in rats: Role of nitric oxide and cytokines. *Life Sciences*, *67*(18), 2247–2256.

Bellin, M. F. S. Z., Auberton, E., Sarfati, G., Duron, J. J., Khayat, D., & Grellet, J. (1994). Liver metastases: Safety and efficacy of detection with superparamagnetic iron oxide in MR imaging. *Radiology*, *193*(3), 657–663.

Bucak, S., Jones, D. A., Laibinis, P. E., & Hatton, T. A. (2003). Protein separations using colloidal magnetic nanoparticles. *Biotechnology Progress*, *19*(2), 477–484.

Butoescu, N., Jordan, O., Burdet, P., Stadelmann, P., Petri-Fink, A., Hofmann, H., et al. (2009). Dexamethasone-containing biodegradable superparamagnetic microparticles for intra-articular administration: Physicochemical and magnetic properties, *in vitro* and *in vivo* drug release. *European Journal of Pharmaceutics and Biopharmaceutics*, *72*(3), 529–538.

Butoescu, N., Seemayer, C., Palmer, G., Guerne, P-A., Gabay, C., Doelker, E., et al. (2009). Magnetically retainable microparticles for drug delivery to the joint: Efficacy studies in an antigen-induced arthritis model in mice. *Arthritis Research and Therapy*, *11*(3), 1–10.

Caruso, R. A., & Antonietti, M. (2001). Sol–gel nanocoating: An approach to the preparation of structured materials. *Chemistry of Materials*, *13*(10), 3272–3282.
Chastellain, M., Petri, A., & Hofmann, H. (2004). Particle size investigations of a multistep synthesis of PVA coated superparamagnetic nanoparticles. *Journal of Colloid and Interface Science*, *278*(2), 353–360.
Corot, C., Robert, P., Idée, J.-M., & Port, M. (2006). Recent advances in iron oxide nanocrystal technology for medical imaging. *Advanced Drug Delivery Reviews*, *58*(14), 1471–1504.
Gupta, A. K., & Gupta, M. (2005). Synthesis and surface engineering of iron oxide nanoparticles for biomedical applications. *Biomaterials*, *26*(18), 3995–4021.
Haaksman, I. K., Besemer, A. C., Jetten, J. M., Timmermans, J. W., & Slaghek, T. M. (2006). The oxidation of the aldehyde groups in dialdehyde starch. *Starch/Stärke*, *58*(12), 616–622.
Harisinghani, M. G., Barentsz, J., Hahn, P. F., Deserno, W. M., Tabatabaei, S., van de Kaa, C. H., et al. (2003). Noninvasive detection of clinically occult lymph-node metastases in prostate cancer. *New England Journal of Medicine*, *348*(25), 2491–2499.
He, C., Hu, Y., Yin, L., Tang, C., & Yin, C. (2010). Effects of particle size and surface charge on cellular uptake and biodistribution of polymeric nanoparticles. *Biomaterials*, *31*(13), 3657–3666.
Laurent, S., Forge, D., Port, M., Roch, A., Robic, C., Vander Elst, L., et al. (2008). Magnetic iron oxide nanoparticles: Synthesis, stabilization, vectorization, physicochemical characterizations, and biological applications. *Chemical Reviews*, *108*(6), 2064–2110.
Lee, K., Kim, S.-G., Kim, W.-S., & Kim, S. (2002). Properties of iron oxide particles prepared in the presence of dextran. *Korean Journal of Chemical Engineering*, *19*(3), 480–485.
Lin, C.-L., Lee, C.-F., & Chiu, W.-F. (2005). Preparation and properties of poly(acrylic acid) oligomer stabilized superparamagnetic ferrofluid. *Journal of Colloid and Interface Science*, *291*(2), 411–420.
Liu, D., Wu, W., Ling, J., Wen, S., Gu, N., & Zhang, X. (2011). Effective PEGylation of iron oxide nanoparticles for high performance *in vivo* cancer imaging. *Advanced Functional Materials*.
Lu, Y., Yin, Y., Mayers, B. T. b., & Xia, Y. (2002). Modifying the surface properties of superparamagnetic iron oxide nanoparticles through a sol–gel approach. *Nano Letters*, *2*(3), 183–186.
Massia, S. P., & Stark, J. (2001). Immobilized RGD peptides on surface-grafted dextran promote biospecific cell attachment. *Journal of Biomedical Materials Research*, *56*(3), 390–399.
Mehvar, R. (2000). Dextrans for targeted and sustained delivery of therapeutic and imaging agents. *Journal of Controlled Release*, *69*(1), 1–25.
Mislovičová, D., Masárová, J., & Gemeiner, P. (2001). Study of interaction of mannan-BSA neoglycoconjugates with concanavalin A. *Artificial Cells, Blood Substitutes and Biotechnology*, *29*(4), 335–345.
Munnier, E., Cohen-Jonathan, S., Linassier, C., Douziech-Eyrolles, L., Marchais, H., Soucé, M., et al. (2008). Novel method of doxorubicin–SPION reversible association for magnetic drug targeting. *International Journal of Pharmacology*, *363*(1–2), 170–176.
Neenu, S., Gareth, J. S. J., Romisa, A., & Shareen, H. D. (2010). Potential toxicity of superparamagnetic iron oxide nanoparticles (SPION). *Nano Reviews*, 1.
Petri-Fink, A., Chastellain, M., Juillerat-Jeanneret, L., Ferrari, A., & Hofmann, H. (2005). Development of functionalized superparamagnetic iron oxide nanoparticles for interaction with human cancer cells. *Biomaterials*, *26*(15), 2685–2694.
Raach, A., & Reiser, O. (2000). Sodium chlorite–hydrogen peroxide—A mild and selective reagent for the oxidation of aldehydes to carboxylic acids. *Journal fur Praktische Chemie*, *342*(6), 605–608.
Ran, N., Singha, K., Yu, M.-K., Jon, S. Y., Kim, Y. S., Ahn, Y. K., et al. (2010). Hybrid superparamagnetic iron oxide nanoparticle-branched polyethylenimine magnetoplexes for gene transfection of vascular endothelial cells. *Biomaterials*, *31*(14), 4204–4213.
Raynal, I., Prigent, P., Peyramaure, S., Najid, A., Rebuzzi, C., & Corot, C. (2004). Macrophage endocytosis of superparamagnetic iron oxide nanoparticles: Mechanisms and comparison of ferumoxides and ferumoxtran-10. *Investigative Radiology*, *39*(1), 56–63.
Reimer, B., & Tombach., P. (1998). Hepatic MRI with SPIO: Detection and characterization of focal liver lesions. *European Radiology*, *8*(7), 1198–1204.
Reimer, P., & Balzer, T. (2003). Ferucarbotran (Resovist): A new clinically approved RES-specific contrast agent for contrast-enhanced MRI of the liver: Properties, clinical development, and applications. *European Radiology*, *13*(6), 1266–1276.
Schöpf, B., Neuberger, T., Schulze, K., Petri, A., Chastellain, M., Hofmann, M., et al. (2005). Methodology description for detection of cellular uptake of PVA coated superparamagnetic iron oxide nanoparticles (SPION) in synovial cells of sheep. *Journal of Magnetism and Magnetic Materials*, *293*(1), 411–418.
Shen, T., Weissleder, R., Papisov, M., Bogdanov, A., & Brady, T. J. (1993). Monocrystalline iron oxide nanocompounds (MION): Physicochemical properties. *Magnetic Resonance in Medicine*, *29*(5), 599–604.
Vu-Quang, H., Muthiah, M., Lee, H. J., Kim, Y. K., Rhee, J. H., Lee, J. H., et al. (2012). Immune cell-specific delivery of beta-glucan-coated iron oxide nanoparticles for diagnosing liver metastasis by MR imaging. *Carbohydrate Polymers*, *87*(2), 1159–1168.
Vu-Quang, H., Yoo, M. K., Jeong, H. J., Lee, H. J., Muthiah, M., Rhee, J. H., et al. (2011). Targeted delivery of mannan-coated superparamagnetic iron oxide nanoparticles to antigen-presenting cells for magnetic resonance-based diagnosis of metastatic lymph nodes *in vivo*. *Acta Biomaterialia*, *7*(11), 3935–3945.
Yamaura, M., Camilo, R. L., Sampaio, L. C., Macêdo, M. A., Nakamura, M., & Toma, H. E. (2004). Preparation and characterization of (3-aminopropyl)triethoxysilane-coated magnetite nanoparticles. *Journal of Magnetism and Magnetic Materials*, *279*(2–3), 210–217.
Yoo, M. K., Kim, I. Y., Kim, E. M., Jeong, H.-J., Lee, C. M., Jeong, Y. Y., et al. (2007). Superparamagnetic iron oxide nanoparticles coated with galactose-carrying polymer for hepatocyte targeting. *Journal of Biomedicine and Biotechnology*, 1–9.
Yoo, M. K., Park, I. Y., Kim, I. Y., Park, I. K., Kwon, J. S., Jeong, H. J., et al. (2008). Superparamagnetic iron oxide nanoparticles coated with mannan for macrophage targeting. *Journal of Nanoscience and Nanotechnology*, *8*(10), 5196–5202.
Yu, S., & Chow, G. M. (2004). Carboxyl group ($-CO_2H$) functionalized ferrimagnetic iron oxide nanoparticles for potential bio-applications. *Journal of Materials Chemistry*, *14*(18), 2781–2786.
Zhao, H., & Heindel, N. (1991). Determination of degree of substitution of formyl groups in polyaldehyde dextran by the hydroxylamine hydrochloride method. *Pharmaceutical Research*, *8*(3), 400–402.